Comparative Medicine
Copyright 2005
by the American Association for Laboratory Animal Science

Vol 55, No 6
December 2005
Pages 510-514

Murine Xenograft Model of *Spirocerca lupi*-Associated Sarcoma

Noa Stettner,[1] Eyal Ranen,[2] Gillian Dank,[2] Eran Lavy,[2] Itamar Aroch,[2] Shimon Harrus,[2] Ori Brenner,[1] and Alon Harmelin[1,*]

Nodular masses and granulomas of the esophagus are among the most frequent lesions caused by *Spirocerca lupi*, a nematode parasite of dogs, and neoplastic transformation of these granulomas to osteosarcoma or fibrosarcoma has been described. In this study, we developed a xenograft murine model of *S. lupi*-associated sarcoma. Samples of esophageal fibrosarcoma and osteosarcomas were excised from three dogs diagnosed with spirocercosis. These sarcomas were inoculated into three groups of 6-week-old NOD/SCID mice to create three tumor lines of *S. lupi*-associated sarcomas. Mice in all groups developed tumors after inoculation, and the cell lines could be further propagated as second-generation xenografts. We successfully established xenograft murine models of three different lines of *S. lupi*-associated sarcoma that offer readily available sources of these tumors for further experiments. This resource will facilitate studies on the malignant transformation of the granulomas, establishment of efficient chemotherapy and radiotherapy regimens, and identification of diagnostic molecular markers.

The nematode *Spirocerca lupi* is primarily a parasite of dogs, but other carnivores may be infected. The adult *S. lupi* is found in a nodular mass in the wall of the host's thoracic esophagus. The female lays embryonated eggs that are excreted in the host's feces. Eggs are ingested by the intermediate host, corprophagus beetles, and develop to infective larva stage. The primary hosts are infected by ingestion of these beetles or of a variety of transport hosts including birds, reptiles, amphibians, and small mammals. In carnivore hosts, infective larvae penetrate the gastric mucosa and migrate within the walls of the gastric arteries to the thoracic aorta. About 3 months postinfection, the larvae leave the aorta and migrate to the esophagus, where they complete their development over the next 3 months while inducing a granulomatous reaction (2, 5, 15). Esophageal granulomas and tumors, aortic scars, and aortic aneurysms are the most frequent lesions associated with this parasite (5, 11, 16). Neoplastic transformation of esophageal granulomas to osteosarcomas or fibrosarcomas has been noted in infected dogs, and the incidence of these tumors increases significantly in areas endemic to *S. lupi* (2, 16, 18, 22). Metastases are frequently present in the lungs, lymph nodes, heart, liver, and kidneys (1).

The pathogenesis of *S. lupi*-associated neoplasia is unknown (9). Reactive fibroblasts exhibiting numerous mitotic figures have been described to occur in early granulomatous lesions (2). The intense inflammatory reaction in these lesions is suspected to result in vigorous fibroblast proliferation that can lead to malignant transformation, as is postulated for feline injection-site sarcomas and ocular sarcomas after chronic uveitis and trauma (13, 21). Recently it was suggested that bone marrow-derived cells, which frequently are recruited to sites of tissue injury and inflammation, represent a potential source of malignancy (7). Another suggestion is that an oncogenic stimulus, such as a chemical, viral, or metabolic product of the parasite or an environmental agent, is involved in this neoplastic transformation (2, 9).

Definitive diagnosis of spirocercosis is made by detecting the typical eggs in fecal smears or by floatation (14) or by visualizing the parasite in typical lesions (5). The presence of typical esophageal granulomas by endoscopy and of spondylitis of the caudal thoracic vertebrae in thoracic radiographs are considered pathognomonic (2, 4, 18). Clinical diagnosis of esophageal tumors can be made by either radiography or endoscopy, but both methods may not lead to definitive diagnosis. Radiographically, it is impossible to differentiate tumors from other opaque soft tissue masses (18). Neoplasia is suspected when mass mineralization or pulmonary metastases are present (4). Endoscopy is considered more specific and sensitive (15). It allows direct visualization of the mass surface, which can be helpful in differentiating a tumor from a granuloma. Whereas granulomas typically present as broad-based protuberances with a nipple-like orifice, tumors are usually irregular, protrude through the esophageal mucosa, are pedunculated or cauliflower-like, and have areas of necrosis and discoloration (18). However, the endoscopic findings can be variable, and advanced granulomas may mimic neoplasms (15). Endoscopic biopsies of esophageal masses may not support differentiation between a tumor and a granuloma because of false-negative results (3, 4, 18).

Treatment options for esophageal tumors include surgical excision, chemotherapy, and radiation (23). Esophageal surgery is difficult and is associated with frequent perioperative and postoperative complications (10, 12). Often the procedure is not feasible due to extensive or multiple lesions or both (5). The prognosis for dogs with esophageal sarcomas is reported to be poor (23). However, the use of advanced diagnostic and surgical techniques has prolonged the median survival by months and has resulted in improvement in patients' quality of life (18, 19). Chemotherapy is used as an adjunctive palliative treatment of soft tissue sarcomas after surgical removal, and doxorubicin-

Received: 5/24/05. Revision requested: 9/23/05. Accepted: 10/01/05.
Department of Veterinary Resources, Weizmann Institute of Science, Rehovot, Israel[1]; Koret School of Veterinary Medicine, The Hebrew University of Jerusalem, Rehovot, Israel[2].
[*]Corresponding author.

http://prime-pdf-watermark.prime-prod.pubfactory.com/ | 2025-02-26

Table 1. Signalment and clinical history of the donor dogs and gross and microscopic features of the source tumors

	Line 1	Line 2	Line 3
Age (years)	6	9	8
Gender	Castrated male	Female	Spayed female
Breed	Mixed	Mixed	Labrador retriever
Macroscopic description	6-cm esophageal mass	7-cm esophageal mass	Multiple 10- to 15-cm esophageal masses
Histology	Fibrosarcoma—neoplastic spindle cells forming whorls, giant cells, and cartilage islands; low mitotic rate	Osteosarcoma—neoplastic spindle cells and osteoblasts, giant cells, and osteoid depostion	Osteosarcoma—neoplastic spindle cells and osteoblasts with osteoid depostion
Metastasis	Pulmonary	Pulmonary	Not detected
Survival	Euthanized 5 months postoperatively	Died during surgery	Died due to surgical complications 1 day postoperatively

based protocols have been shown to be the most effective (13). To date, however, there are no available data on the effectiveness of chemotherapy in the treatment of spirocercosis-associated esophageal sarcomas (18).

In the present study, we established a xenograft murine model of *Spirocerca lupi*-associated sarcoma. The stages in the development of this model are described and its applications are discussed.

Materials and Methods

Animals. All experiments were performed according to standard protocols (17) and were approved by the Weizmann Institutional Animal Care and Use Committee.

Two strains of mice were used in this study: NOD.CB17-*Prkdc*^{scid}/J (NOD/SCID from the specific pathogen-free colony of the Department of Veterinary Resources of the Weizmann Institute of Science [Rehovot, Israel]) and C57BL/6JOlaHsd (Harlan Laboratories, Jerusalem, Israel). Mice (age, 6 weeks; male and female) were anesthetized for the surgical procedure by using a mixture of ketamine HCl (Fort Dodge, Iowa) 200 mg/kg intraperitoneally and xylazine HCl (V.M.D. Arendonk, Belgium) 10 mg/kg intraperitoneally. During the experimental period, mice were housed in a room on a 12:12-h light:dark cycle in individually ventilated cages containing wood shavings and were given autoclaved laboratory rodent chow and acidified sterile water ad libitum. They were housed five animals per cage in a specific pathogen-free facility according to recommendations by the Federation of European Laboratory Animal Science Associations. Mice were monitored daily for development of any adverse reactions in response to the tumor, which were measured with calipers twice weekly. The mice were observed until tumors reached an average diameter of 1.5 cm (< 10% of body weight) or until tumors began to ulcerate, after which mice were euthanized. Autopsy and histopathologic analysis was performed on each animal.

Sample collection and initial cell transfer. Tumor samples were obtained during esophageal surgery from three different dogs admitted to the Hebrew University Veterinary Teaching Hospital and diagnosed with *S. lupi*-associated sarcoma after detection of typical esophageal masses by using endoscopy. The diagnosis was confirmed by histologic examination in all three cases. The signalment of the dogs and macroscopic and microscopic descriptions of their tumors are presented in Table 1.

After surgical excision, tumor samples were placed in Hartmann's solution (Laboratoire Aguettan, Lyon, France) and cut with scissors into ~2-mm-diameter pieces. Three groups, each consisting of 10 6-week-old NOD/SCID mice, were inoculated with a different source of *S. lupi*-associated sarcoma by subcutaneous transplantation into the right flank.

Mouse antibody production test (MAP). The xenografted sarcoma tumor was excised under sterile conditions and placed in Hartmann's solution (Laboratoire Aguettan, Lyon, France). The tissue was minced with scissors to small fragments and gently homogenized mechanically through a wire membrane. The number of detectable viable cells was minute, not allowing an accurate cell count. Cells and debris were resuspended in lactated ringer's solution. For each tumor line, five 6-week-old C57BL/6JOlaHsd mice were injected with sarcoma suspension subcutaneously and intraperitoneally (0.5 ml each site), and five additional mice served as controls. The mice were euthanized 5 weeks later, and blood samples were collected. Sera were tested serologically for antibody production against a panel of pathogens, including mouse hepatitis virus, pneumonia virus of mice, Sendai virus, ectromelia virus, *Mycoplasma pulmonis*, mouse encephalomyelitis virus, *Helicobacter* sp., cilia-associated respiratory bacillus, K virus, epizootic diarrhea of infant mice virus, reovirus 3, lymphocytic choriomeningitis virus, mouse cytomegalovirus, polyomavirus, mouse adenovirus, and *Bacillus piliformis* by using immunofluorescent antibody tests and enzyme-linked immunofluroescence assays (Charles River Laboratories, Wilmington, Mass.).

Preparation of cell suspension. A xenografted sarcoma tumor, 1.5 cm in diameter, was excised under sterile conditions and placed in Hartmann's solution (Laboratoire Aguettan, Lyon, France). The tissue was minced with scissors to small fragments and gently homogenized mechanically through a wire membrane. The number of detectable viable cells was minute, not allowing an accurate cell count. Cells and debris were resuspended in Hartmann's solution. Three groups, each consisting of 10 6-week-old NOD/SCID mice, were injected subcutaneously with 0.5 ml of sarcoma cell suspension from a single tumor line. The procedure was repeated for the next generation of xenograft.

Histopathology. Samples were fixed in 10% neutral buffered formalin, processed routinely, embedded in paraffin, sectioned at 4 to 5 μm, and stained with hematoxylin and eosin (H&E).

Results

MAP test. The MAP tests of all three lines was negative for the 17 pathogens, thus allowing us to introduce these cell lines into our specific pathogen-free unit.

Tumor development in mice. Tumors were well tolerated by the mice. There were no tumor-related deaths, and none of the mice experienced overt adverse effects due to tumor transplanta-

http://prime-pdf-watermark.prime-prod.pubfactory.com/ | 2025-02-26

Table 2. Clinical, macroscopic, and microscopic characteristics of xenograft tumors

Line	1	2	3
Detection time (weeks)[a]	4	3	6
Number of mice that developed tumors[b]	6	6	5
Growth rate (mm diameter/week)	80	50	1–2
Time to maximal tumor size (weeks)[c]	2	3–4	12–16
Macroscopic appearance	Smooth, multinodular pale pink masses with connective-tissue consistency	Multinodular, smooth, pale pink, and hard masses	Nodular smooth, pale pink, and hard masses
Necrosis or ulceration?	No	No	Yes, central necrosis
Invasive tumor?	No	Yes	No
Metastasis	None detected	None detected	None detected
Number of mice that developed second-generation xenografts	10	8	7
Growth rate of second- generation xenograft	Same as first-generation	Same as first-generation	Same as first-generation
Current passage number	5	4	2
Tumor behavior at current passage	Growth rate increases with each passage; tumor now detected at 2–3 weeks and reaches 1.5 mm in 10 days.	Tumors maintain original growth rate	Tumors maintain original growth rate

[a]Time from transplantation to development of a small, visible lump.
[b]n = 10 per group.
[c]Average time from transplantation to tumor 1.5 cm in diameter.

tion. Growth and morphology data on the three xenograft tumor lines are presented in Table 2.

Histopathology. The histologic features of the original tumors (Fig. 1, A through C) were preserved after xerotransplantation into mice (Fig. 1, D through F). The three tumors differed in their appearance by light microscopy. Line 1 (Fig. 1, A and D) resembled a typical fibrosarcomatous growth. In particular, neoplastic cells consisted of a uniform population of spindle and oval cells arranged in densely cellular fascicles, forming chevron and storiform patterns. Neoplastic cells had small to moderate amounts of eosinophilic to amphophillic cytoplasm and finely granular to vesicular oval nuclei, with one or more nucleoli. The rate of mitotic figures was ~1 to 2/high-power field (HPF), and the amount of collagen deposition was variable.

Lines 2 (Fig. 1, B and E) and 3 (Fig. 1, C and F) were more heterogeneous in appearance. In addition to fibroblastic elements, they contained sheets of oval to irregular neoplastic cells with distinct cytoplasmic outlines and round to irregular vesicular nuclei, consistent with osteoblasts. Mineralized and nonmineralized osteoid deposits were present, indicating that these tumors were osteosarcomas. Osteoid trabeculae were abundant in Line 2 but sporadic in Line 3. Multinucleated giant cells, consistent with osteoclasts were present in Line 2. The mitotic rate was ~4/HPF for Line 2 and ~6/HPF for Line 3.

Discussion

Research to define cell transformation and tumorigenesis has proceeded at a rapid pace, although there are still gaps in our knowledge (9). The mechanism of tumor induction continues to be one of the most intriguing and challenging elements in the pathogenesis of *S. lupi*-associated sarcomas (2, 5). The main aim of the present study was to develop a murine model of *S. lupi*-associated sarcoma to facilitate further studies of its unique pathogenesis and to allow research into improved diagnostic and treatment modalities.

Inoculation of *S. lupi*-associated sarcoma cells into NOD/SCID mice resulted in reliable tumor development in all three groups. These tumors can be maintained by passage as viable xenografts and thus can be used as a readily available source for further experiments.

The three tumor lines showed differences in tumor appearance, growth rate, histology, and degree of malignancy. Line 1 was a typical fibrosarcoma and showed the most aggressive behavior. It had the fastest growth rate, which increased with each passage. Line 2 was a moderately aggressive osteosarcoma, with a slower growth rate compared with Line 1, and has maintained its growth rate to date. Despite its slower growth rate, it penetrated the abdominal wall, indicating invasive behavior, thus making it more difficult to treat by surgical excision. Line 3 also was an osteosarcoma but was the least aggressive of the three tumors, and its progression was the slowest. This tumor also has maintained its growth rate upon passage. This diversity in tumor behavior among the three lines offers an advantage for further studies and allows comparison among different tumor types, degrees of malignancy, and growth rates.

In all three lines, there was no evidence of tumor metastasis, although the source tumors of Lines 1 and 2 led to pulmonary metastases. Because of the rapid growth rate of these tumors, mice had to be euthanized when tumors reached 1.5 cm in diameter at 2 to 3 weeks (Line 1) or 3 to 4 weeks (Line 2) after tumors were detected. The possibility that metastases would have developed had tumor growth continued cannot be excluded.

The NOD/SCID mice strain was the most appropriate for this study. This strain, which is homozygous for a spontaneous mutation for severe combined immune deficiency, is characterized by an absence of functional T and B lymphocytes, lymphopenia, hypogammaglobulinemia, a normal hematopoietic microenvironment, and impaired antigen-presenting cells and macrophage activity, as well as impaired function of natural killer cells. NOD/SCID mice accept allogeneic and xenogeneic grafts, making them

http://prime-pdf-watermark.prime-prod.pubfactory.com/ | 2025-02-26

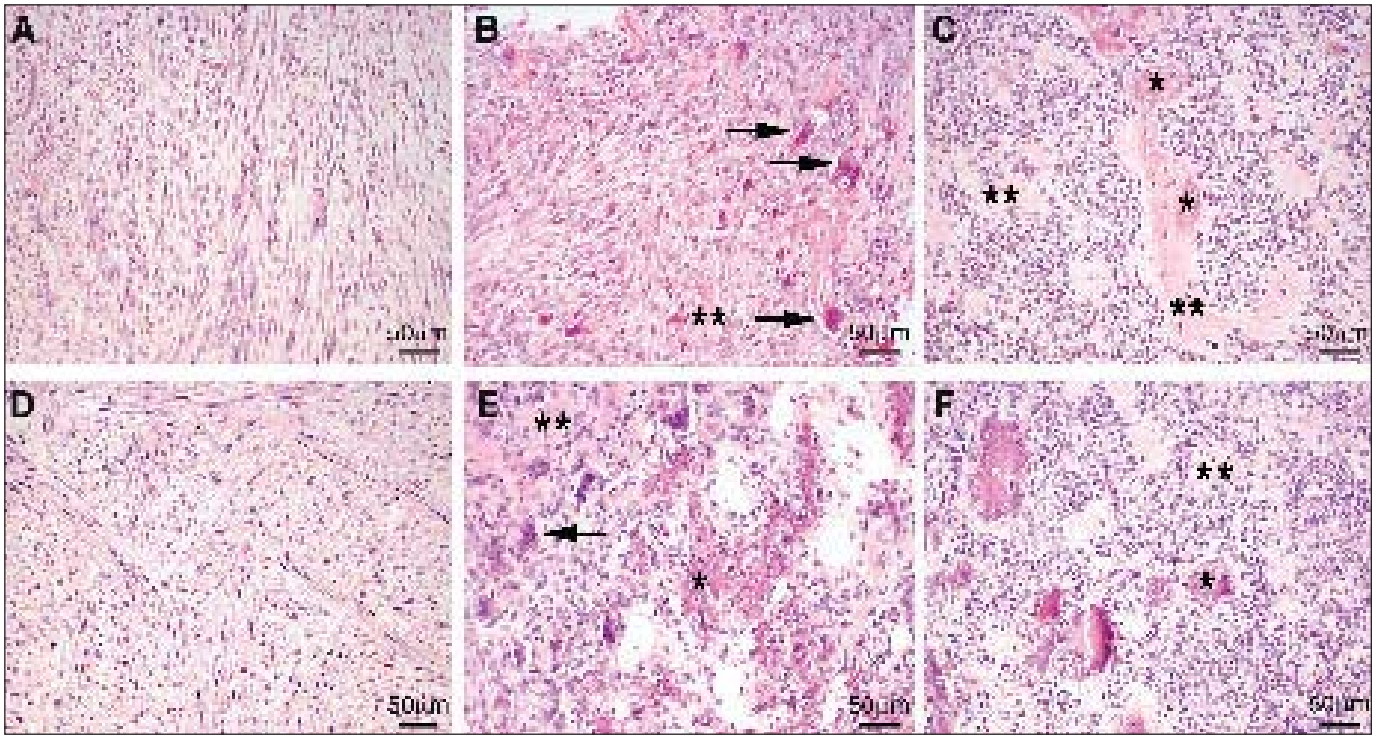

Figure 1. Histologic features of original canine (A through C) and xenograft (D, Line 1; E, Line 2; F, Line 3) *S. lupi*-associated sarcomas. (A and D) Fibrosarcoma with typical interlacing fascicles of spindle cells. (B and E) Osteosarcoma with deposition of neoplastic osteoid. Black arrows, osteoclasts; *, mineralized osteoid; **, nonmineralized osteoid. (C and F) Osteosarcoma. *, Mineralized osteoid; **, nonmineralized osteoid. H&E stain; bar, 50 µm.

an ideal model for cell transfer experiments (6, 8).

This model presents several advantages for the study of *S. lupi*-associated sarcoma. First, esophageal tumors are rare in dogs and account for 0.5% of reported tumors only (20). In the naturally occurring disease, it takes about 6 months for esophageal granulomas to develop postinfection (9). Neoplastic transformation occurs only in some cases and may occur as long as several years postinfection. This protracted and unpredictable course makes research of the naturally occurring disease complex. A model of esophageal sarcoma facilitates further studies by providing a readily available tumor source.

Second, diagnosis of *S. lupi*-associated sarcoma based on endoscopic biopsies is tentative, as differentiation of tumor versus granuloma may be impossible (3, 4, 18). Many cases present with late-stage disease, which limits treatment options. In the NOD/SCID model, the lack of host immune response against the tumor yields a relatively pure population of sarcoma cells. This feature will facilitate characterization of the neoplastic cells by cytogenetic and immunohistochemical methods in the hope of finding specific markers which could be used for early diagnosis in the future.

One of the most fascinating aspects of S. *lupi* infection is the induction of neoplastic transformation. A third advantage of our NOD/SCID mouse model is that it reproduces the main features of the natural behavior of canine *S. lupi*-associated sarcoma. This characteristic may facilitate studies of mechanisms of tumor transformation, including the transformation of inflammatory reaction to neoplasia, a topic of much current interest (7). Finally, because surgical excision of esophageal masses is highly complicated, often impossible, and frequently leads to poor results, our murine model can be used for further studies of alternative treatments including chemotherapy, radiotherapy, and their combination with surgical excision.

In conclusion, in this study we successfully created three lines of canine *S. lupi*-associated sarcoma that differed in their appearance, growth rate, histologic features, and degree of malignancy in a mouse model. This model provides a readily available and reproducible tumor source. It is our hope that this model will enable further studies of the pathogensis, diagnosis, and treatment of canine *S. lupi*-associated sarcoma.

References

1. **Aiello, S. E.** 1998. *Spirocerca lupi* infection, p. 683-684. *In* The Merck veterinary manual, 8th ed. Merck & Co., Whitehouse Station, N.J.
2. **Bailey, W. S.** 1972. *S. lupi*: a continuing inquiry. J. Parasitol. **58:**3-22.
3. **Berry, W. L.** 2000. *S. lupi* esophageal granulomas in 7 dogs: resolution after treatment with doramectin. J. Vet. Intern. Med. **15:**609-612.
4. **Dvir, E., R. M. Kirberger, and D. Malleczek.** 2001. Radiographic and computed tomographic and clinical presentation of spirocercosis in the dog. Vet. Radiol. Ultrasound. **42:**119-129.
5. **Fox, S. M., J. Burns, and J. Hawkins.** 1988. Spirocercosis in dogs. Compend. Cont. Educ. Pract. Vet. **10:**807-822.
6. **Greiner, D. L. and L. D. Shultz.** 1998. The use of NOD/SCID mice in biomedical research, p. 173-203. *In* E. Leiter and M. Atkinson (ed.), NOD mice and related strains: research applications in diabetes, AIDS, cancer and other diseases. R. G. Landes Co., Austin, Tex.
7. **Houghton, J., C. Stoicov, S. Nomura, A. B. Rogers, J. Carlson, H. Li, X. Cai, J. G. Fox , J. R. Goldenring, and T. C. Wang.** 2004. Gastric cancer originating from bone marrow-derived cells. Science **26:**1568-1571.

http://prime-pdf-watermark.prime-prod.pubfactory.com/ | 2025-02-26

8. **The Jackson Laboratory.** 2005. Web databases. [Online]. Available at http://jaxmice.jax.org/info/index.html. Accessed 5/10/05.
9. **Johnson, R. C. A.** 1992. Canine spirocercosis and associated esophageal sarcoma. Compend. Cont. Educ. Pract. Vet. **15:**577–580.
10. **Kyles, A. E.** 2002. Esophagus, p. 573–592. *In* D. Slatter (ed.), Textbook of small animal surgery, 3rd ed. Saunders, Philadelphia.
11. **Lavy, E. S. Harrus, M. Mazaki-Tovi, H. Bark, A. Markovics, A. Hagag, I. Aizenberg, and I. Aroch.** 2003. *Spirocerca lupi* in dogs: prophylactic effect of doramectin. Res. Vet. Sci.**75:**217-222.
12. **Lemarie, R. J. and G. Hosgood.** 1998. Esophagotomy and esophageal anastomosis, p. 193–197. *In* M. J. Bojrab, G. W. Ellison, and B. Slocum (ed.), Current techniques in small animal surgery, 4th ed. Williams and Wilkins, Baltimore, Md.
13. **MacEwen, E.G., B. E. Powers, D. Macy, and S. J. Withrow.** 2001. Soft tissue sarcomas, p. 283-304. *In* S. J. Withrow and E. G. MacEwen (ed.), Small animal clinical oncology, 3rd ed. Saunders, Philadelphia.
14. **Markovics, A. and B. Medinski.** 1996. Improved diagnosis of low intensity *Spirocerca lupi* infection by the sugar flotation method. J. Vet. Diagn. Invest. **8:**400-401.
15. **Mazaki-Tovi, M., G. Baneth, I. Aroch, S. Harrus, P. H. Kass, T. Ben-Ari, G. Zur, I. Aizenberg, H. Bark, and E. Lavy.** 2002. Canine spirocercosis: clinical, diagnostic, pathological, and epidemiologic characteristics. Vet. Parasitol. **107:**235–250.
16. **Moulton, J.E.** 1978. Tumors of the alimentary tract in the dog, p. 252-258. *In* J. E. Moulton (ed.), Tumors in domestic animals, 2nd ed. University of California Press, Berkeley, Calif.
17. **National Research Council.** 1996. Guide for the care and use of laboratory animals. National Academy Press, Washington, D.C.
18. **Ranen, E., E. Lavy, I. Aizenberg, S. Perl, and S. Harrus.** 2004. Spirocercosis-associated esophageal sarcomas in dogs. A retrospective study of 17 cases (1997-2003). Vet. Parasitol. **119:**209-221.
19. **Ranen, E., M. H. Shamir, R. Shahar, and D. E. Johnston.** 2004. Partial esophagectomy with single layer closure for treatment of esophageal sarcomas in 6 dogs. Vet. Surg. **33:**428-434.
20. **Ridgeway, R. L. and P. F. Suter.** 1979. Clinical and radiographic signs in primary and metastatic esophageal neoplasms of the dog. J. Am. Vet. Med. Assoc. **174:**700-704.
21. **Seguin, B.** 2002. Injection site sarcomas in cats. Clin. Tech. Small Anim. Pract. **17:**168-173.
22. **Seibold, H. R., W. S. Bailey, and B. F. Hoerlein.** 1955. Observations on the possible relation of malignant esophageal tumors and *S. lupi* lesions in the dog. Am. J. Vet. Res. **16:**5-14.
23. **Withrow, S. J.** 2001. Esophageal cancer, p. 320-321. *In* S. J. Withrow and E. G. MacEwen (ed.), Small animal clinical oncology, 3rd ed. Saunders, Philadelphia.

http://prime-pdf-watermark.prime-prod.pubfactory.com/ | 2025-02-26